Two-dimensional fuel regression simulations with level set method for hybrid rocket internal ballistics

Yuki Funami*

Faculty of Engineering, Kanagawa University, 3-27-1 Rokkakubashi, Kanagawa-ku, Yokohama-shi, Kanagawa, 221-8686, Japan

Abstract. Low fuel regression rate is the main drawback of hybrid rocket which should be overcome. One of the improvement techniques to this problem is usage of a solid fuel grain with a complicated geometry port, which has been promoted owing to the recent development of additive manufacturing technologies. In the design of a hybrid rocket fuel grain with a complicated geometry port, the understanding of fuel regression behavior is very important. Numerical investigations of fuel regression behavior requires a capturing method of solid fuel surface, i.e. gas-solid interface. In this study, level set method is employed as such a method and the preliminary numerical tool for capturing a hybrid rocket solid fuel surface is developed. At first, to test the adequacy of the numerical modeling, the simulation results for circular port are compared to the experimental results in open literature. The regression rates and oxidizer to fuel ratios show good agreements between the simulations and the experiments, after passing enough time. However, during the early period of combustion, there are the discrepancies between the simulations and the experiments, owing to transient phenomena. Second, the simulations of complicated geometry ports are demonstrated. In this preliminary step, a star shape is employed as complicated geometry of port. The slot number effect in star port is investigated. The regression rate decreases with increasing the slot number, except for the star port with many slots (8 slots) in the latter half of combustion. The oxidizer to fuel ratio increases with increasing the slot number.

Keywords: hybrid rocket; fuel surface regression; level set method; numerical simulation

1. Introduction

Hybrid rocket is one of the attractive candidates for future space propulsion. It has the propellants in the different phases; typically, the oxidizer in the liquid phase and the fuel in the solid phase. The oxidizer and fuel are physically isolated before starting combustion, leading to the intrinsic safety of hybrid rocket. The safety promotes the applications of hybrid rocket to commercial human space flights, such as SpaceShipTwo planed by Virgin Galactic (Ribeiro and Greco Jr. 2011), and to students' rocket projects (Nakasuka 2009).

The mechanism characterizing hybrid rocket is the turbulent boundary layer combustion. The oxidizer is fed into the port of the solid fuel grain and mixed with the gasified fuel within the boundary layer. Subsequently the oxidizer and fuel react and the flame is formed. The heat transfer from the flame to the solid fuel surface promotes the gasification of the solid fuel. Through these

---

*Corresponding author, Assistant Professor, E-mail: funami-yuki@kanagawa-u.ac.jp

processes, the mechanism of the boundary layer combustion is self-sustained. It is dominated by the diffusion process of the oxidizer and gasified fuel within the boundary layer. This causes that the flame locates relatively far from the fuel surface and that the fuel regression rate becomes low.

Low fuel regression rate is the main drawback of hybrid rocket. Some improvement methods of this problem were proposed by many researchers. For example, fuel additive (Karabeyoglu 2017), swirling oxidizer flow injection (Yuasa *et al.* 1999), low melting point fuel (Karabeyoglu *et al.* 2001) and so on. Owing to the recent development of additive manufacturing technologies, another improvement technique, solid fuel grain with a complicated geometry port, has been studied. There have been proposed various port geometries, such as star swirl port (Fuller *et al.* 2011, Armold *et al.* 2013, Zhang *et al.* 2016), helical port (Whitmore *et al.* 2015, Whitmore and Walker 2017), star fractal port and cherry blossom fractal port (Tateyama and Takano 2017). The complicated geometry port has some advantages on improving the regression rate. It is because 1) its high friction resistance promotes laminar-turbulent transition, leading to increase the heat transfer rate to the solid fuel surface, 2) its large surface area gives high mass flow of the gasified fuel from the solid fuel surface and 3) if the port has a helical or swirl geometry, it generates swirling flow.

In the design of a hybrid rocket fuel grain with a complicated geometry port, the understanding of fuel regression behavior is very important. A solid fuel surface can be considered as a gas-solid interface. A numerical investigation of fuel regression behavior hence requires a capturing method of gas-solid interface. Level set method is such a capturing method. This method had been employed for calculating burning surface regression behavior of solid rocket. The burning surface of solid rocket can be also considered as gas-solid interface. Qin *et al.* (2006) simulated the burning surface with a crack and the surface of an inhomogeneous grain. Albarado *et al.* (2012) developed the higher order integration scheme with level set method for solid rocket motor simulation. Sullwald *et al.* (2013) proposed the combined method of the burning surface regression simulation and the solid rocket internal ballistics analysis. These studies may suggest the application of level set method to hybrid rocket fuel regression simulation.

In this study, the preliminary numerical tool for capturing a hybrid rocket solid fuel surface is developed with level set method. At first, to test the adequacy of the numerical modeling, the simulation results for circular port grain will be compared to the experimental results in open literature. Next, the simulations of complicated geometry ports will be demonstrated. In this preliminary step, a classical star shape is employed as complicated geometry of port. The slot number effect in star port grain will be investigated numerically.

2. Numerical modeling and methods

Hybrid rocket fuel regression simulation requires a capturing method of gas-solid interface. In this research, fuel regression behavior is simulated with the level set method (Osher and Fedkiw 2003) on a two-dimensional plane perpendicular to the axial direction of fuel grain port.

2.1 Definition of level set function

In the level set method, a variable ϕ called *level set function* is introduced. The level set function is defined as a signed distance function. The absolute value of this function means the distance from the interface. Hence there is the interface on the location where the level set function is equal to zero. Two regions of different phase are separated by the interface. The sign of level set

function at a point means which region the point belongs to. In order to model a hybrid rocket fuel grain, the region of positive level set function is defined as hybrid rocket solid fuel, while the region of negative level set function is defined as combustion gas.

Time evolution of the interface is simulated by solving the advection equation for level set function.

$$\frac{\partial \phi}{\partial t} + \mathbf{v} \cdot \nabla \phi = \mu \Delta \phi \tag{1}$$

The artificial viscous term is added to the equation for numerical stability. The artificial viscosity is set to be proportional to the square of computational cell size (Chang *et al.* 1996).
Eq. (1) is discretized with finite difference method. The convection term of Eq. (1) is evaluated by second order ENO (Essentially Non-Oscillatory) scheme (Shu and Osher 1989, Harten 1989, Chang *et al.* 1996). The artificial viscous term is evaluated by second order centered difference scheme (Chang *et al.* 1996). Boundary conditions are set by first order extrapolation. Time integration is second order Adams-Bashforth method.

2.2 Advection velocity of level set function

Advection velocity needs to be evaluated when solving the advection equation for level set function, Eq. (1). The behavior of the interface which has zero level set function corresponds to that of the solid fuel surface, provided that the advection velocity is equal to the fuel regression rate at the interface. The advection speed should hence satisfy two constraints; 1) the absolute value of advection velocity is the same as that of fuel regression rate, 2) the advection velocity has the direction normal to the interface and from the gas phase to the solid phase. As the result, the advection velocity of level set function is given as follows.

$$\mathbf{v} = \dot{r} \frac{\nabla \phi}{|\nabla \phi|} \tag{2}$$

From the point of view of physics, fuel regression rate is determined by the heat balance at the solid fuel surface. This mechanism requires a coupling analysis of thermal and fluid dynamics for estimating fuel regression rate. However, for simplicity, the fuel regression rate is evaluated by the empirical correlation, Eq. (3), in this study.

$$\dot{r} = a G_o^{\ n} \tag{3}$$

The oxidizer mass flux is determined by as follows

$$G_o = \frac{\dot{m}_o}{A_p} \tag{4}$$

Oxidizer mass flow rate is usually set to constant in experiments. In this study, the oxidizer mass flow rate is dealt as a constant. The port cross-sectional area is determined by using the level set function.

$$A_p = \int_A \left(1 - H_\varepsilon \right) dA \tag{5}$$

$$H_\varepsilon = \begin{cases} 0 & \text{at } \phi < -\varepsilon \\ \dfrac{\phi + \varepsilon}{2\varepsilon} + \dfrac{1}{2\pi}\sin\left(\dfrac{\pi\phi}{\varepsilon}\right) & \text{at } |\phi| \le \varepsilon \\ 1 & \text{at } \phi > \varepsilon \end{cases} \tag{6}$$

Here, A is total area of calculation domain, H_ε is approximated Heaviside function, ε is minimal value (it is set to the same value of computational cell size). Using Eqs. (2)-(6), the advection velocity of level set function can be evaluated.

2.3 Reinitialization of level set function

As mentioned in Section 2.1, the level set function is defined as a distance function from the interface. However the level set function gradually losses the nature of distance function as Eq. (7) during calculation process. In order to maintain the level set function as a distance function without changing the interface of zero level set function, the level set function should be reinitialized.

$$|\nabla \phi| = 1 \tag{7}$$

The reinitialization method proposed by Sussman *et al.* (1999) is employed in this study. This method is divided into three steps; 1) the value of level set function ϕ is copied into a variable d, 2) in order to give the variable d the nature of distance function as Eq. (7), the following equation for pseudo-time τ is solved,

$$\frac{\partial d}{\partial \tau} = S(\phi)\left(1 - |\nabla d|\right) \tag{8}$$

$$S(\phi) = \begin{cases} -1 & \text{if } \phi < 0 \\ 0 & \text{if } \phi = 0 \\ 1 & \text{if } \phi > 0 \end{cases} \tag{9}$$

3) the value of level set function ϕ is replaced with that of the variable d obtained by solving Eq. (8).

When solving Eq. (8), the equation is rewritten as the same form as advection equation.

$$\frac{\partial d}{\partial \tau} + \mathbf{w} \cdot \nabla d = S(\phi) \tag{10}$$

$$\mathbf{w} = S(\phi)\frac{\nabla d}{|\nabla d|} \tag{11}$$

Eq. (10) is discretized with finite difference method. The convection term of Eq. (10) is evaluated by second order ENO scheme. Boundary conditions are set by first order extrapolation. Time integration is second order Runge-Kutta method.

As found from Eq. (9), it is implicitly imposed that the values of level set function at the interface do not change. However, it is known that, due to discretization, the location of the interface moves during the reinitialization process (Tsubogo *et al.* 2003). In order to avoid this

problem, Tsubogo *et al.* (2003) proposed that the reinitialization is not performed in the region satisfying Eq. (12). In this study, this approach is employed.

$$|\phi| \leq 0.5h \tag{12}$$

Here *h* is computational cell size.

2.4 Estimation of oxidizer to fuel ratio

Oxidizer to fuel ratio is one of the important parameters related to rocket performance. Especially in hybrid rocket, it changes with time, because port area opens up with the fuel grain gasified, leading to decrease oxidizer mass flux and to decrease fuel regression ratio as found from Eq. (3), in other words, to decrease fuel mass flow rate. A designer of hybrid rocket requires the understanding of the behavior of oxidizer to fuel ratio. Hence oxidizer to fuel ratio is estimated by using the result of level set simulation in this study.

In the estimation of oxidizer to fuel ratio, it is assumed that instantaneous port geometry and fuel regression rate is uniform along the port axis at every moment during combustion period. The oxidizer to fuel ratio is estimated by using the level set function.

$$\text{O/F} = \frac{\dot{m}_o}{\dot{m}_f} \tag{13}$$

$$\dot{m}_f = \rho_f \dot{r} l_p L \tag{14}$$

$$l_p = \int_A \delta_\varepsilon dA \tag{15}$$

$$\delta_\varepsilon = \begin{cases} \dfrac{1}{2\varepsilon}\left\{1+\cos\left(\dfrac{\pi\phi}{\varepsilon}\right)\right\} & \text{at } |\phi| \leq \varepsilon \\ 0 & \text{otherwise} \end{cases} \tag{16}$$

Here, l_p is perimeter of port cross-section, L is port length, δ_ε is approximated Delta function.

3. Simulations of circular port with comparison to experiments in open literature

The uniform fuel regression rate along the port axis is assumed as mentioned in Section 2.4. In other words, it can be considered that the space-averaged fuel regression rate is used as a local value at every location. This space-averaged but instantaneous fuel regression rate is determined by using the empirical correlation, Eq. (3), in this study. However this correlation is generally obtained by using experimental data about not only space-averaged but also time-averaged fuel regression rate and oxidizer mass flux. It is also assumed that the instantaneous fuel regression rate can be approximated by the value obtained from the correlation. In this section, to test the adequacy of this assumption, the simulation results for circular port grain will be compared to the experimental results obtained by Shanks and Hudson (1994).

Table 1 Oxidizer mass flow rates in the experiments performed by Shanks and Hudson (1994)

Grain number	Run number	Oxidizer mass flow rate [kg/s]
1	1	0.0735
1	2	0.0635
1	3	0.0544
1	4	0.0467
2	1	0.0798
2	2	0.0608*
2	3	0.0540
2	4	0.0458
3	1	0.0780
3	2	0.0594
3	3	0.0526
3	4	0.0454
4	1	0.0508
4	2	0.0449
4	3	0.0355
4	4	0.0336
4	5	0.0262
4	6	0.0187
5	1	0.0563
5	2	0.0481
5	3	0.0413
5	4	0.0338
5	5	0.0261
5	6	0.0185
6	1	0.0522
6	2	0.0449
6	3	0.0375
6	4	0.0334
6	5	0.0265
6	6	0.0183

*The original value in the literature is corrected here

3.1 Numerical settings of the circular port simulations

Shanks and Hudson (1994) performed the hybrid rocket combustion experiments using gaseous oxygen (GOX) and hydroxyl-terminated polybutadiene (HTPB). Six fuel grains with a circular port were used. These grains had the same length as 25.4 cm and the same initial port diameter as 19.1 mm. Each grain was combusted during 3 seconds either four or six times. The oxidizer mass flow rate in each firing is listed in Table 1. After each firing, averaged fuel regression rate was

determined by using the weighed fuel mass loss. On the other hand, instantaneous fuel regression rate was not measured and a time history of fuel regression rate was not obtained in this test series. However approximated time histories of fuel regression rate were obtained with the following procedure. In this procedure, after a certain grain was burned and the fuel regression rate of it was determined, the burned grain was burned and evaluated again. This was repeated using each grain. Run number in Table 1 is how many times a certain grain was burned and, hence, means *discrete time* approximately. Though the fuel regression rate at each run number is time-averaged and space-averaged, the time histories of fuel regression rate can be approximately obtained owing to multiple successive firings. The empirical correlation, Eq. (17), was obtained from the results of this test series.

$$\dot{r} = 0.0401 G_o^{0.674} \tag{17}$$

In Eq. (17), the unit of fuel regression rate is mm/s and the unit of oxidizer mass flux is kg/m^2/s.

In this section, four or six times successive firings are simulated at each grain. The numerical settings, such as fuel and oxidizer material, grain port geometry before firing, combustion duration and oxidizer mass flow rate, are set to the same as the experiments. The parameters in Eq. (3) is set to a=0.0.401 and n=0.674 which is the same as Eq. (17). It is noted again that the unit of fuel regression rate is mm/s and the unit of oxidizer mass flux is kg/m^2/s in Eqs. (3) and (17). The calculation domain has 60 mm×60 mm size with a 512×512 equally-spaced orthogonal computational mesh. The discrete time interval is set to 0.005 s.

3.2 Numerical results of the circular port simulations

Under the same conditions of the Shanks and Hudson's experiments, numerical simulations of fuel surface regression were performed with the level set method. In the level set method, the time evolution of the level set function is captured. The zero level set function expresses a solid fuel surface at each time. The time evolutions of the surface in the cases of grain number 3 and 6, as representative cases, are shown in Fig. 1. The black circle means the initial surface before combustion. The instantaneous surfaces are shown every 1 second from inside to outside. The color of the lines means run number, hence red is run number (R. No.) 1, blue R. No. 2, yellow R. No. 3, green R. No. 4, pink R. No. 5, purple R. No. 6. As one can see in Fig. 1, in both cases of grain number 3 and 6, the fuel port increases in size while maintaining its shape and the rate of surface regression decreases with time.

Time- and space-averaged port cross-sectional area, fuel regression rate and oxidizer to fuel ratio at each run is calculated from the numerical results in the same manner of the experiments. These values are compared to the experimental ones, as shown in Figs 2-4. It is noted again that run number, which is the horizontal axis in these figures, means discrete time approximately. In the case of grain number 6, though there are small differences between the simulations and experiments at run number 1 and 2, the numerical values of these parameters are considered to coincide with the experimental ones. In Fig. 2, the port cross-sectional area increases with increasing the run number which practically corresponds to time. As one can see from Eqs. (3)-(4), the oxidizer mass flux decreases with increasing the port cross-sectional area, hence the fuel regression rate decreases as shown in Fig. 3. The oxidizer to fuel ratio decreases slightly with increasing the run number in Fig. 4. On the other hand, there are some discrepancies in the case of grain number 3. Fig. 3 shows that the fuel regression rate of the numerical result is much higher

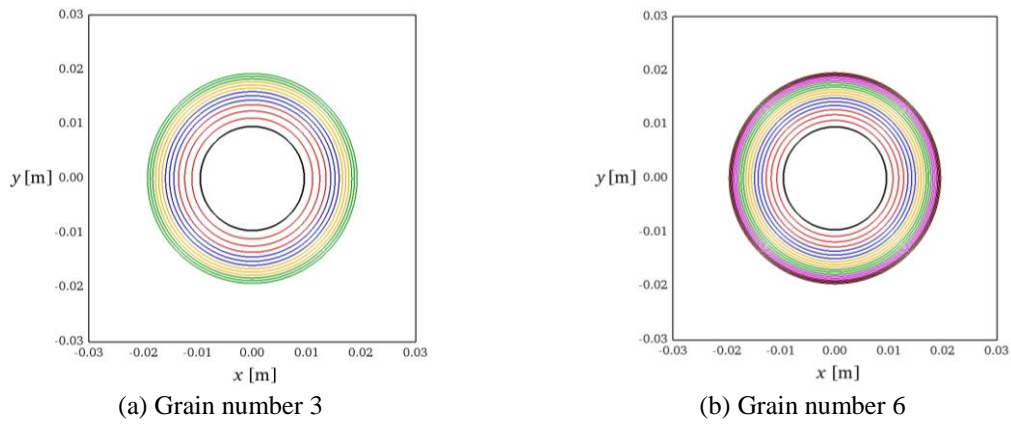(a) Grain number 3   (b) Grain number 6

Fig. 1 Time evolutions of the surface. From inside to outside, black: initial state, red: run number (R. No.) 1, blue: R. No. 2, yellow: R. No. 3, green: R. No. 4, pink: R. No. 5, purple: R. No. 6
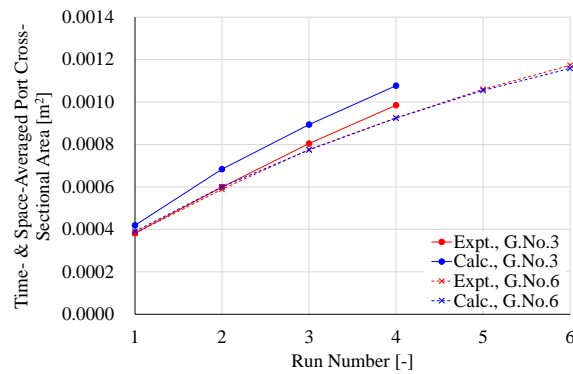

Fig. 2 Port cross-sectional area in the cases of grain number (G. No.) 3 and 6
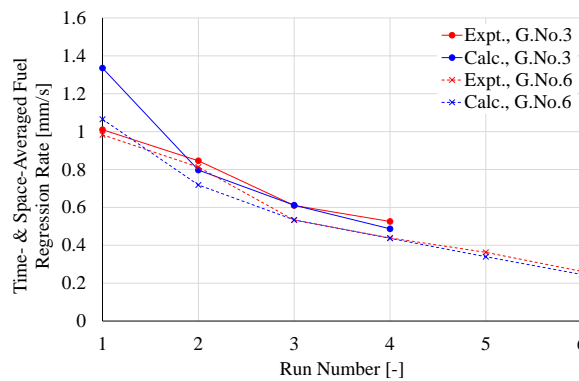

Fig. 3 Fuel regression rate in the cases of grain number (G. No.) 3 and 6

than that of the experimental result at run number 1. After run number 2, the difference of fuel regression rate between the simulations and experiments almost diminishes. Owing to the initial discrepancy of fuel regression rate, the port cross-sectional area of the numerical result is larger
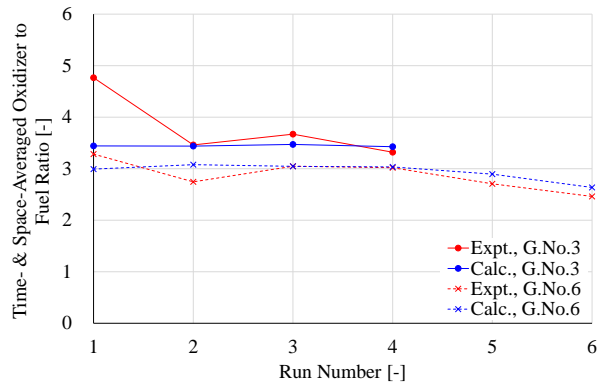
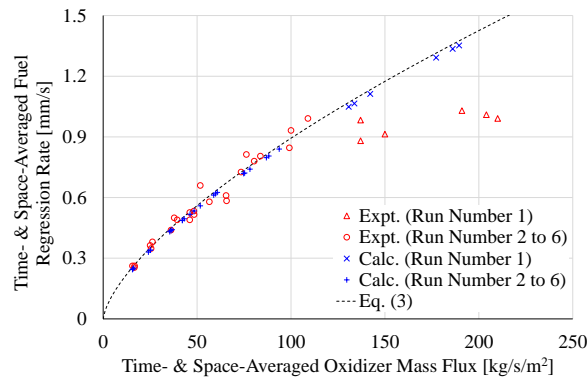Fig. 4 Oxidizer to fuel ratio in the cases of grain number (G. No.) 3 and 6

Fig. 5 All data about fuel regression rate including grain number 1 to 6

than that of the experimental result at run number 1 and the difference of port cross-sectional area is subsequently maintained after run number 2, as shown in Fig. 2. In Fig. 4, the oxidizer to fuel ratio of the numerical result is much smaller than that of the experimental result at run number 1. The difference of oxidizer to fuel ratio after run number 2 is less apparent than that at run number 1.

All data of the numerical and experimental results including grain number 1 to 6 are plotted in Fig. 5. The discrepancy of fuel regression rate at run number 1 mentioned above is also found clearly as one can see in Fig. 5. In the experiments, the dependency of fuel regression rate on oxidizer mass flux changes after the run number 2 firings. Shanks and Hudson (1994) pointed out that the effect of char layer generated during the run number 1 firings may cause the change of the fuel regression rate dependency. In these simulations, this char layer effect is not introduced and hence this discrepancy arises. The transient phenomena, such as char layer formation, need to be modeled and implemented for getting a more accurate method.

4. Numerical investigation of the slot number effect in star port grain

In this section, the simulations of complicated geometry ports are demonstrated with using the

Table 2 Initial port size and operational condition in the case of the circle with no slot

Fuel	HTPB
Oxidizer	GOX
Port diameter	20 mm
Port cross-sectional area	314 mm^2
Port length	25.0 cm
Grain surface area	157 cm^2
Oxidizer mass flow rate	0.060 kg/s
Combustion duration	20 s

Table 3 Port length in the case of the star port

Slot number [-]	3	4	5	6	8
Port length [cm]	9.06	7.83	6.97	6.34	5.42

developed level set approach. In this preliminary step, a classical star shape is employed as complicated geometry of port. The star shape is composed of a center circle and radial slots. The slot number effect in star port grain is investigated numerically.

4.1 Numerical settings of the star port simulations

In this investigation of star port grain, the engine scale and operational condition is set to be comparable to that of a lab-scale engine as Shanks and Hudson's experiments. The solid fuel grains have a classical star shape port and the number of radial slot is parametrically changed in the range of 0 to 8 except for 1, 2 and 7. The initial shapes of star port are shown in Fig. 6 as a black line. The 0 slot port, that is, circular port is a reference shape. The engine scale and operational condition in the simulation of the circle with no slot is summarized at Table 2. On the other hand, in the star port grains, both port diameter and port length are set, provided that both port cross-sectional area and grain surface area are the same as those of the circular port grain. The port length is summarized at Table 3. The other settings, that is, fuel, oxidizer, oxidizer mass flow rate and combustion duration, are given the same as the circular port grain. Hence the initial regression rates and initial oxidizer to fuel ratios have no difference between the circular port grain and the star port grains. This means that the effect of port shape, i.e. slot number, on time histories about hybrid rocket parameters is investigated in this section.

Solid fuel is HTPB and oxidizer is GOX in these simulations. The fuel regression rate law is expressed as Eq. (3). The preconstant *a* and exponent *n* in Eq. (3) is assumed to be the same value as that in Shanks and Hudson's experiments. In other words, Eq. (17) is also used here.

The calculation domain has 80mm×80mm size with a 512×512 equally-spaced orthogonal computational mesh. The discrete time interval is set to 0.005 s.

4.2 Numerical results of the star port simulations

The star port simulations were done with using the developed level set approach. Tracking the location of the zero level set functions means capturing the solid fuel surface deformation. The

(a) Circle with no slot

(b) 3 star (circle with 3 slots)

(c) 4 star (circle with 4 slots)

(d) 5 star (circle with 5 slots)

(e) 6 star (circle with 6 slots)
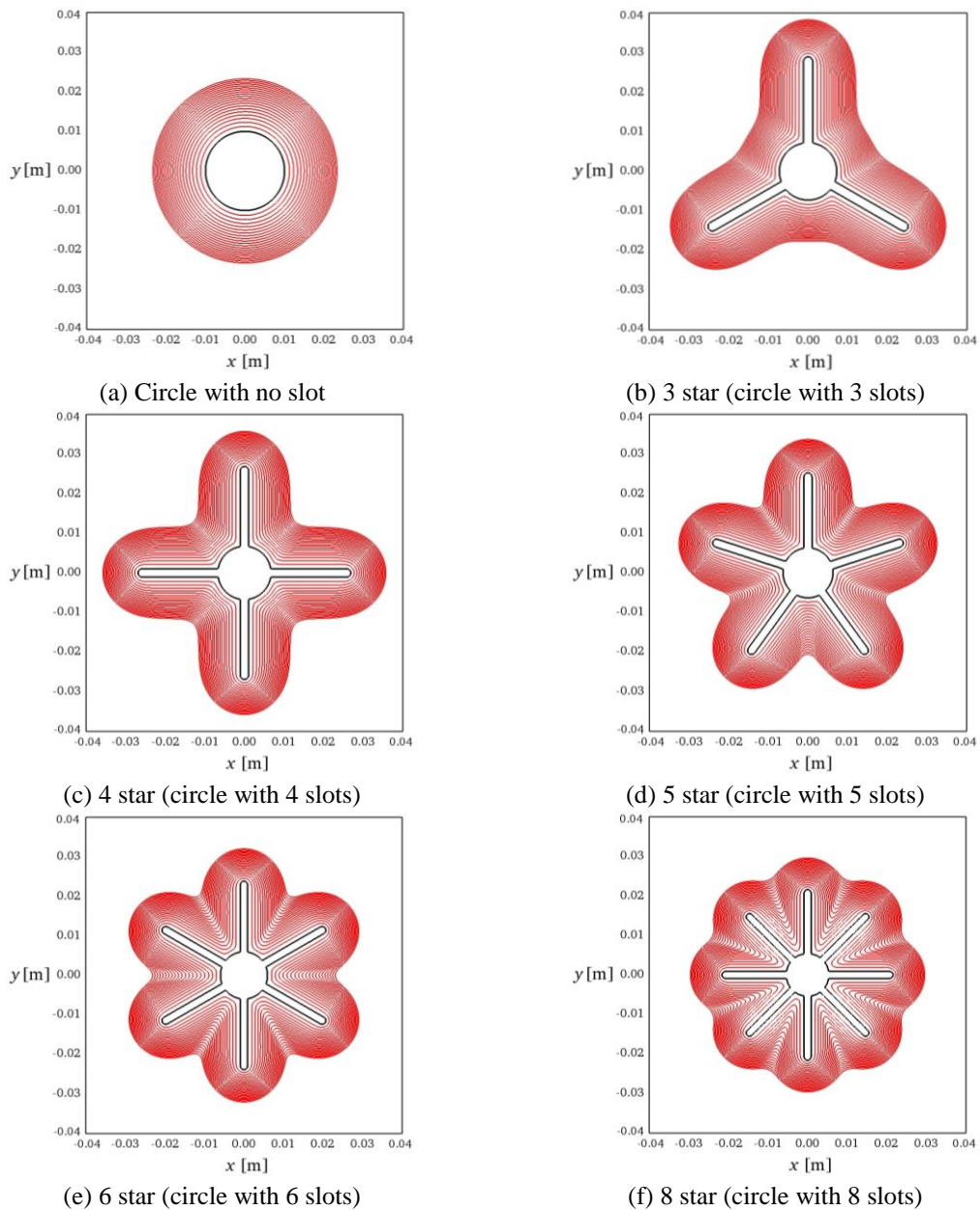
(f) 8 star (circle with 8 slots)

Fig. 6 Time evolutions of the surface in the star port grains. The black line is the initial surface

time evolutions of the surface in the star port grains are shown in Fig. 6. The black curve means the initial solid fuel surface before combustion. The instantaneous surfaces expressed by the red curves are shown every 1 second from inside to outside. As one can see in Fig. 6, the port opens up with time. The consumption of the fuel portions between the slots gradually makes the port shape circular. This tendency is accentuated especially in the star port with many slots such as the 8 star port in Fig. 6(f).
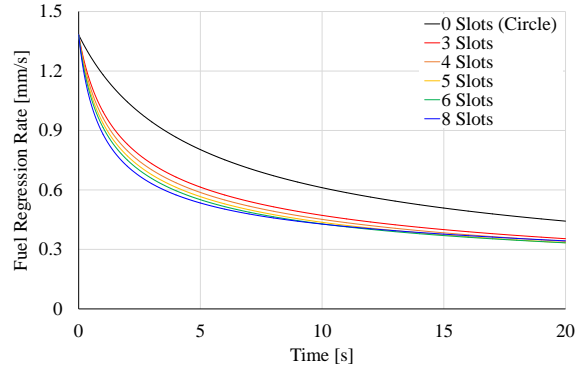
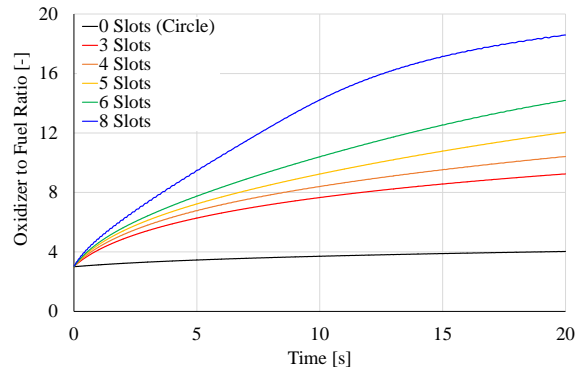Fig. 7 Fuel regression rates of the star ports

Fig. 8 Oxidizer to fuel ratios of the star ports

The time histories of fuel regression rate are shown in Fig. 7. The regression rate decreases with time in all cases. In the range of 0 to 6 slots, it decreases with increasing the slot number. In the early period of combustion, the regression rate for the 8 star port grain has the lowest value in all cases. However, after almost the middle of time, the fuel regression rate for the 8 star port grain becomes higher than that for the 6 and 5 star port grain. This cause relates to the variation of the port shape. Fuel regression rate is determined by Eq. (3). Assuming oxidizer mass flow rate as a constant in these simulations, Eq. (3) can be rewritten as follows.

$$\dot{r} = a_A A_p^{-n} \tag{18}$$

$$a_A \equiv a\dot{m}_o^{\,n} = \text{const.} \tag{19}$$

Hence fuel regression rate is inversely proportional to the *n*-th power of port cross-sectional area. It is also found from Eq. (18) that the decreasing rate of fuel regression rate depends on the increasing rate of port cross-sectional area. The increasing rate of port cross-sectional area in the star port grains are higher than that in the circular port. It is because, while the fuel surface of the circular port regresses in the radial direction, that of the star ports regresses not only in the radial direction but also in the circumferential direction around the slots of the star ports. The slots are, however, gradually disappeared owing to the fuel consumption. After consuming the large fuel

portions between the slots of the star ports, the fuel surface regression is in almost the same manner of the circular port grain, that is, in the radial direction only. The fuel surface regression gets into this situation more rapidly with increasing the slot number of the port, because the initial fuel portions between the slots become smaller with increasing the slot number.

The time histories of oxidizer to fuel ratio are shown in Fig. 8. The oxidizer to fuel ratio increases with time in all cases. While the fuel regression rate decreases with time as mentioned above, the grain surface area increases as shown in Fig. 6. Fig. 8 means that decreasing the fuel regression rate has the bigger impact on the oxidizer to fuel ratio than increasing the grain surface area. As one can see in Fig. 8, the oxidizer to fuel ratio increases with increasing the slot number. The fuel regression rate decreases with increasing the slot number (except for the 8 star port in the latter half of combustion). This effect appears in the time histories of oxidizer to fuel ratio.

The oxidizer to fuel ratio for the star port grains is very high, compared to the ratio for the circular port grain, as shown in Fig. 8. The main reason of this is a short length of the star ports. In order to set the same initial port cross-sectional area and initial grain surface area as those of the circular port grain, the port length of the star ports is changed in every case, as shown at Table 3. For example, the port length of the 8 star port is 5.42 cm, while that of the circular port is 25.0 cm. If the port length is set longer, the oxidizer to fuel ratio can be decreased and approached to the appropriate value for the practical use.

5. Conclusions

The preliminary numerical tool for capturing a hybrid rocket solid fuel surface was developed with using the level set method. In this tool, capturing the zero level set function leads to simulating the solid fuel surface deformation. The advection velocity of level set function, i.e. the fuel regression rate, is evaluated with the well-known empirical correlation. This correlation is obtained by using space- and time-averaged data in experiments. It is also assumed in this tool that the instantaneous fuel regression rate can be approximated by the value evaluated from the correlation. At first, to check the adequacy of this assumption, the simulation results for circular port grain were compared to the experimental data in the open literature. The fuel regression rates and oxidizer to fuel ratios show good agreements between the simulations and the experimental data, after passing enough time (run number 2 to 6). During the early period of combustion (run number 1), however, there are the discrepancies between the simulations and the experimental data, owing to transient phenomena.

Second, in order to demonstrate the feasibility of the developed tool for complicated geometry port analysis, the simulations of the star ports were performed. In these simulations, the slot number effect in star port grain was evaluated. As shown in the numerical results, the fuel regression rate decreases with increasing the slot number of star port, except for the 8 star port in the latter half of combustion. The different tendency of the 8 star pot is caused by the variation of the port shape from star shape to circular shape. The oxidizer to fuel ratio increases with increasing the slot number, because of the decrease of the fuel regression rate.

For future applications of this numerical tool to more practical problems, two improvements will be needed as follow.

For getting more accuracy in simulations, the local and instantaneous evaluation of fuel regression rate will be required. One of such evaluation approaches is the use of the empirical correlation for the local and instantaneous fuel regression rate. This approach is a simple extension

of the tool in this study. Another approach is reactive fluid and thermal simulation coupled with level set method for surface capturing. While the phenomena in a combustion chamber can be described in detail, the computational cost of this approach is high and the application of it to parametric study is very difficult.

In order to apply this developed tool to the analysis of three-dimensionally complicated geometry ports such as a star swirl port, the extension of the tool from two-dimension to three-dimension will be also required. It can be accomplished easily by using the three-dimensional advection equation for level set function.

References

Albarado, K., Shelton, A. and Hartfield, R.J. (2012), "SRM simulation using the level set method and higher order integration schemes", *Proceedings of the 48th AIAA/ASME/SAE/ASEE Joint Propulsion Conference and Exhibit*, Atlanta, Georgia, U.S.A., July.

Armold, D., Boyer, J.E., Kuo, K.K., DeSain, J.D., Curtiss, T.J. and Fuller, J.K. (2013), "Test of hybrid rocket fuel grains with swirl patterns fabricated using rapid prototyping technology", *Proceedings of the 49th AIAA/ASME/SAE/ASEE Joint Propulsion Conference*, San Jose, California, U.S.A., July.

Chang, Y.C., Hou, T.Y., Merriman, B. and Osher, S. (1996), "A level set formulation of Eulerian interface capturing methods for incompressible fluid flows", *J. Comput. Phys.*, **124**(2), 449-464. https://doi.org/10.1006/jcph.1996.0072.

Fuller, J., Ehrlich, D., Lu, P., Jansen, R. and Hoffman, J. (2011), "Advantages of rapid prototyping for hybrid rocket motor fuel grain fabrication", *Proceedings of the 47th AIAA/ASME/SAE/ASEE Joint Propulsion Conference and Exhibit*, San Diego, California, U.S.A., July.

Harten, A. (1989), "ENO schemes with subcell resolution", *J. Comput. Phys.*, **83**(1), 148-184. https://doi.org/10.1016/0021-9991(89)90226-X.

Karabeyoglu, A. (2017*), Performance Additives for Hybrid Rockets*, in *Rocket Propulsion, A Comprehensive Survey of Energetic Materials*, Springer, Switzerland.

Karabeyoglu, M.A., Cantwell, B.J. and Altman, D. (2001), "Development and testing of paraffin-based hybrid rocket fuels", *Proceedings of the 37th AIAA/ASME/SAE/ASEE Joint Propulsion Conference and Exhibit*, Salt Lake City, Utah, U.S.A., July.

Nakasuka, S. (2009), "Students' challenges towards new frontier –enlarging activities of UNISEC and Japan universities", *Trans. JSASS Space Tech. Japan*, **7**(ists26), To_1_1-To_1_6.

Osher, S. and Fedkiw, R. (2003), *Level Set Methods and Dynamic Implicit Surfaces,* Springer, New York, U.S.A.

Qin, F., Guoqiang, H., Peijin, L. and Jiang, L. (2006), "Algorithm study on burning surface calculation of solid rocket motor with complicated grain based on level set methods", *Proceedings of the 42nd AIAA/ASME/SAE/ASEE Joint Propulsion Conference and Exhibit*, Sacramento, California, U.S.A., July.

Ribeiro, M.V.F. and Greco Jr., P.C. (2011), "Hybrid rocket motors propellants: A historical approach", *Proceedings of the 21st International Congress of Mechanical Engineering*, Natal, Brazil, October.

Shanks, R.B. and Hudson, M.K. (1994), "The design and control of a labscale hybrid rocket facility for spectroscopy studies", *Proceedings of the 30th AIAA/ASME/SAE/ASEE Joint Propulsion Conference and Exhibit*, Indianapolis, Indiana, U.S.A., June.

Shu, C.W. and Osher, S. (1989), "Efficient implementation of essentially non-oscillatory shock-capturing schemes, II", *J. Comput. Phys.*, **83**, 32-78.

Sullwald, W., Smit, F., Steenkamp, A. and Rousseau, W. (2013), "Solid rocket motor grain burn back analysis using level set methods and Monte-Carlo volume integration", *Proceedings of the 49th AIAA/ASME/SAE/ASEE Joint Propulsion Conference*, San Jose, U.S.A., July.

Sussman, M., Almgren, A.S., Bell, J.B., Colella, P., Howell, L.H. and Welcome, M.L. (1999), "An adaptive level set approach for incompressible two-phase flows", *J. Comput. Phys.*, **148**(1), 81-124.

https://doi.org/10.1006/jcph.1998.6106.

Tateyama, T. and Takano, A. (2017), "Development of CFRP reinforced lightweight hybrid rocket engine", *Proceedings of the 48th JSASS Annual Meeting,* Tokyo, Japan, April (in Japanese).

Tsubogo, K., Asai, K. and Hadano, K. (2003), "Study on numerical calculation for rupture of bubble at water surface by level set method", *J. Appl. Mech. JSCE*, **6**, 201-208 (in Japanese). https://doi.org/10.2208/journalam.6.201.

Whitmore, S.A. and Walker, S.D. (2017), "Engineering model for hybrid fuel regression rate amplification using helical ports", *J. Propul. Power*, **33**(2), 398-407. https://doi.org/10.2514/1.B36208.

Whitmore, S.A., Walker, S.D., Merkley, D.P. and Sobbi, M. (2015), "High regression rate hybrid rocket fuel grains with helical port structures", *J. Propul. Power*, **31**(6), 1727-1738. https://doi.org/10.2514/6.2014-3751.

Yuasa, S., Shimada, O., Imamura, T., Tamura, T. and Yamamoto, K. (1999), "A technique for improving the performance of hybrid rocket engines", *Proceedings of the 35th AIAA/ASME/SAE/ASEE Joint Propulsion Conference and Exhibit*, Los Angeles, California, U.S.A., June.

Zhang, S., Hu, F. and Zhang, W. (2016), "Numerical investigation on the regression rate of hybrid rocket motor with star swirl fuel grain", *Acta Astronautica,* **127**, 384-393. https://doi.org/10.1016/j.actaastro.2016.06.017.

CC

Nomenclature

A total area of numerical domain

A_p port cross-sectional area

a oxidizer mass flux preconstant in the empirical correlation of fuel regression rate

a_A port cross-sectional area preconstant

d alternate variable of level set function in reinitialization process

G_o oxidizer mass flux

H_ε approximated Heaviside function

h computational cell size

L port length

l_p perimeter of port cross-section

$\dot{m}_f$ fuel mass flow rate

$\dot{m}_o$ oxidizer mass flow rate

n oxidizer mass flux exponent in the empirical correlation of fuel regression rate

O/F   oxidizer to fuel ratio

$\dot{r}$ fuel regression rate

S switching function used in reinitialization proces

t time

$\mathbf{v}$ advection velocity of level set function

$\mathbf{w}$ advection velocity of alternate variable of level set function in reinitialization process

δ_ε approximated Delta function

ε minimal value

μ artificial viscosity

ρ_f solid fuel density

τ pseudo-time

ϕ level set function